Research Square

Preprints are preliminary reports that have not undergone peer review.
They should not be considered conclusive, used to inform clinical practice,
or referenced by the media as validated information.

TRIBRID-Optimized MobileNetV3 Framework for Explainable Printed Circuit Board Defect Classification

Manjunath G. Asuti
Visvesvaraya Technological University
Nirmalkumar S. Benni
RNS Institute of Technology
Ramesh B T
ramesh.bt@sitpune.edu.in

Symbiosis Institute of Technology (SIT), Symbiosis International (Deemed University) (SIU)
Phanindra Reddy Kannari
Ballari Institute of Technology & Management
S N Chaitra
NITTE (Deemed to be University, NMAM Institute of Technology (NMAMIT)
K J Kavitha
GM University
B P Mishra
Graphic Era University

Research Article

Keywords: Printed Circuit Board defect classification, Explainable Artificial Intelligence, Grad-CAM, Hyperparameter optimization, MobileNetV3, TRIBRID

Posted Date: July 29th, 2026

DOI: https://doi.org/10.21203/rs.3.rs-10433184/v1

License: This work is licensed under a Creative Commons Attribution 4.0 International License.
Read Full License

Additional Declarations: No competing interests reported.

TRIBRID-Optimized MobileNetV3 Framework for Explainable Printed Circuit Board Defect Classification

[1]Manjunath G. Asuti, [2]Nirmalkumar S. Benni, [3*] Ramesh B T, [4]Phanindra Reddy Kannari, [5]Chaitra S N, [6]Kavitha K J, [7]B P Mishra

[1]Department of Electronics and Communication Engineering, B. N. M. institute of Technology, Bengaluru - 560070, Karnataka, India.

E-mail ID: manjunathasuti@bnmit.in, Orcid Id: https://orcid.org/0000-0001-6577-7396

[2]Department of CSE (AI & ML), RNS Institute of Technology, Bengaluru - 560098, Karnataka, India.

Email Id: nirmalkumarsbenni@rnsit.ac.in, Orcid Id: https://orcid.org/0000-0002-5164-8160

[*3]Symbiosis Institute of Technology (SIT), Symbiosis International (Deemed University) (SIU), Lavale, Pune - 412115, Maharashtra, India.

Email Id: rameshbt049@gmail.com, Orcid Id: https://orcid.org/0000-0003-1370-1538

[4] Department of AI&ML, Ballari Institute of Technology & Management, Ballari-583104, Karnataka, India

Email Id: phanindrareddyk@gmail.com, Orcid Id: https://orcid.org/0000-0002-1764-9661

[5]NITTE (Deemed to be University), NMAM Institute of Technology (NMAMIT), Nitte -574110, Karnataka, India.

Email Id: chaitrasn48@gmail.com, Orcid Id: https://orcid.org/0000-0002-1847-3717

[6]Department of Electronics and Communication Engineering, GM University, Davangere-577006, Karnataka, India.

Email Id: kavithakj219@gmail.com, Orcid Id: https://orcid.org/0000-0002-1819-7919

[7]Department of Electronics and Communication Engineering, Graphic Era University, Dehradun- 248002, Uttarakhand, India.

Email Id: bpmishra435@gmail.com, Orcid Id: https://orcid.org/0000-0002-2369-4266

*Corresponding author: Ramesh B T, Email Id: ramesh.bt@sitpune.edu.in / rameshbt049@gmail.com, Orcid Id: https://orcid.org/0000-0003-1370-1538

Abstract: Printed Circuit Board (PCB) defect inspection is crucial for successful electronic manufacturing, but creating a highly accurate, computationally efficient solution with model interpretability is challenging. This paper introduces an explainable framework for PCB defect classification based on TRIBRID-optimized MobileNetV3. The TRIBRID optimization algorithm automatically tunes the training hyperparameters, and transfer learning is also used to fine-tune the MobileNetV3 model. To offer visual explanations of classification actions, gradient-weighted Class Activation Mapping is also incorporated. Experiments conducted on a publicly available PCB defect set show that the proposed framework outperforms the baseline models, achieving 100.00% accuracy, precision, recall, and F1 score while retaining the lightweight nature of MobileNetV3, which is suitable for intelligent Automated Optical Inspection systems.

Keywords: Printed Circuit Board defect classification; Explainable Artificial Intelligence; Grad-CAM; Hyperparameter optimization; MobileNetV3; TRIBRID.

1. Introduction

Printed Circuit Boards (PCBs) are the mechanical and electrical backbone of modern electronic products, providing mechanical support and electrical connectivity between electronic components. They are used in consumer electronics, automotive systems, industrial automation, medical equipment, aerospace, and communication infrastructures. With the continuous rise of compact, high-performance, and extremely reliable electronic devices, the PCB manufacturing process has become much more complex. Therefore, any defects, regardless of size, can cause electrical failures, product failures, higher maintenance costs, and reduced operational reliability, even if they occur during drilling, etching, soldering, or assembly [1]. It is thus important to properly inspect products before they are brought into service for any surface defects, including missing holes, mouse bites, open circuits, short circuits, spur defects, and spurious copper [2,3].

Traditionally, quality inspection has been carried out by manual visual inspection and Automated Optical Inspection (AOI) systems. Manual inspection is very labor-intensive and time-consuming, and it is susceptible to operator fatigue, which is not suitable in today's high-throughput manufacturing environment [2]. In conventional AOI systems, defects are identified on a surface by applying image processing techniques such as edge detection, thresholding, template matching, and morphological operations to the image. These techniques prove effective in an ideal imaging environment but become problematic when dealing with complex PCB designs, variable lighting, background noise, or the subtle nature of PCB defects [2,4]. This restriction has motivated the creation of intelligent vision-based inspection systems that can extract features from representative images and automatically recognize them from data.

Industrial visual inspection has been revolutionized by the development of Artificial Intelligence (AI), particularly deep learning, which enables leveraging the potential of end-to-end feature extraction and classification. In recent years, Convolutional Neural Networks (CNNs) have proven very successful at learning hierarchical image representations without hand-tuned features, leading to substantial advances in accurately inspecting defects [1,4]. For PCB inspection tasks, several deep learning architectures have been investigated, such as Residual Networks (ResNet), EfficientNet [41], MobileNet, transformer-based models, and attention models [7–10,13,16,18–21]. Publicly available datasets for PCB defects have also helped speed up algorithms by providing a common benchmark and objective comparison among various learning models [5].

Despite advances, deep learning models have not been easily applied in practice in the industrial inspection industry, as these systems should be highly accurate in classification while remaining computationally lightweight. Lightweight convolutional architectures have thus become increasingly popular in real-time inspection applications. In these architectures, MobileNetV3 was an effective trade-off between predictive performance, computational efficiency, and inference speed, especially for resource-limited manufacturing systems [40]. The predictive power of a lightweight model, however, is very sensitive to training hyperparameters such as the learning rate, dropout rate, batch size, and network fine-tuning configuration. These hyperparameters are expensive to determine by hand and often suboptimal [23–29]. Transfer learning has therefore become an effective approach for transferring a pretrained deep learning model to an application-specific dataset to save training time and enhance feature representation and model generalization, especially for limited-labeled datasets [30-34].

Another significant aspect of industrial Artificial Intelligence is the model's interpretability. Deep learning models are often more accurate at predicting the next action. However, they are often black boxes, and the human user does not know what is happening inside the model, which leads to a lack of user trust in a safety-critical industrial application. To address this issue, explainable AI (XAI) methods have been developed that provide visual interpretations of the model's predictions. Gradient-weighted Class Activation Mapping (Grad-CAM) is one of the most popular approaches for highlighting discriminative regions of an image that affect classification decisions, thereby enabling engineers to confirm inspection decisions better and provide increased transparency [35-39].

Although defect inspection of PCBs has achieved tremendous progress, there are still some research challenges. Previous studies have mainly focused on deepening the network [7,13,16,20,21] and generating transformer models, and the attention mechanism has been applied to improve classification performance. However, little attention has been given to smart hyperparameter optimization methods for lightweight transfer learning models, particularly for PCB defect classification. Moreover, explainability is typically used as an additional visualization tool rather than embedded into the inspection workflow. Given these observations, a lightweight, computationally efficient, and easily interpretable framework must be developed to improve classification accuracy with minimal manual effort in hyperparameter tuning.

This paper proposes an explainable framework for the classification of PCB defects using TRIBRID optimized MobileNetV3 to overcome these drawbacks. The backbone classification network used here is MobileNetV3, which is

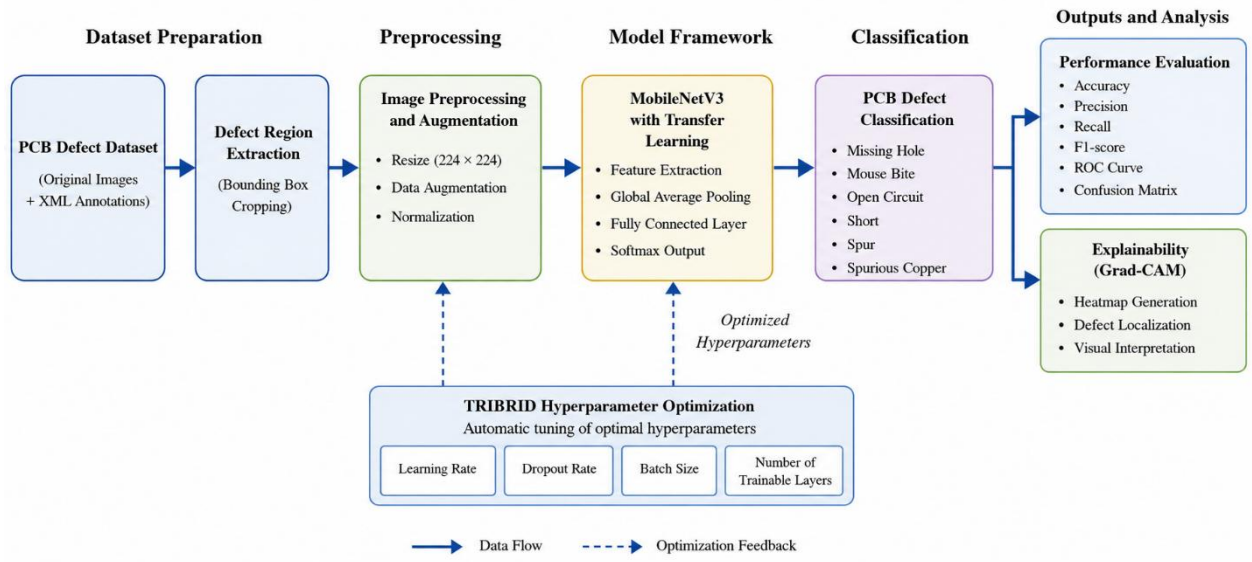


Fig. 1: Workflow of the proposed TRIBRID-optimized MobileNetV3 framework for explainable PCB defect classification.

fine-tuned via transfer learning, while the TRIBRID optimization algorithm [22] is applied to find the optimal hyperparameters automatically. Also, Grad-CAM is embedded to provide a visual explanation of classification decisions, increasing the model's transparency and benefiting industrial inspection applications. The proposed framework is assessed on an open dataset of PCBs, and three other deep neural networks, CNN, ResNet18, and EfficientNet-B0, are comprehensively evaluated and compared to the baseline model, MobileNetV3, as well as compared and ablated.

The salient features of this work are summarized below:

1. To achieve accurate, lightweight defect recognition, a framework for automated PCB defect classification is proposed by combining a MobileNetV3 architecture with transfer learning.
2. The published TRIBRID optimization algorithm automatically determines the hyperparameters of the MobileNetV3 model, eliminating the need for manual selection and improving model efficiency.
3. The effectiveness of the proposed framework is validated using a publicly available PCB defect dataset against a CNN, ResNet18, EfficientNet-B0, and a baseline MobileNetV3 model through a comprehensive comparative evaluation.
4. An ablation study investigates the contribution of the TRIBRID optimization strategy by comparing it with Random Search and Particle Swarm Optimization (PSO) hyperparameter optimization strategies.
5. To improve the interpretability and reliability of the proposed inspection framework for industrial applications, XAI is integrated with Grad-CAM to visualize discriminative defect regions.

The article is divided into the following sections. The methodology proposed is described in Section 2. The experimental setup is detailed in Section 3, Section 4 presents the experimental findings, and Section 5 summarizes the paper.

2. Proposed Methodology

2.1 Overall Framework

The overall workflow of the proposed PCB defect classification is shown in Figure 1. The first step is to prepare the PCB defect dataset by extracting defect regions from the original annotated PCB images using the corresponding bounding-box annotations. The defect patches are cropped and then undergo image preprocessing and data augmentation to diversify the data and improve generalization during training.

Preprocessed images are then fed into a transfer-learning MobileNetV3 classification model. A published TRIBRID optimization algorithm [22] is used to automatically select the best learning rate, dropout rate,
batch size, and network fine-tuning configuration, rather than manually. Optimized hyperparameters are then used to train the MobileNetV3 classifier for PCB defect classification with multiple classes.

Finally, the trained model is evaluated using common classification metrics, including accuracy, precision, recall, F1 score, confusion matrices, and Receiver Operating Characteristic (ROC) analysis. Thus, to make its visualizations more interpretable, Grad-CAM is employed to depict the areas of the image that the model discriminates to make each classification choice. The system is lightweight, automatically optimizes hyperparameters, and integrates XAI into the inspection system, making it suitable for industrial PCB defect automatic classification.

2.2 PCB Defect Dataset and Image Preprocessing

The proposed framework was tested on a publicly available PCB defect dataset comprising six surface defect categories: missing hole, mouse bite, open circuit, short circuit, spur, and spurious copper [5]. Each original PCB image includes XML annotation files that identify defect locations. The defect regions were automatically cropped from the image using the annotated defect region's bounding box coordinates, producing a cropped defect dataset of 2,953 images from 693 annotated PCB samples for ease of image classification. Table 1 presents the distribution of the cropped dataset by class, and Figure 2 shows representative samples of defects.

Images were cropped and resized to 224 × 224 pixels to conform to MobileNetV3's input size. To enhance the

Table 1. Class-wise distribution of the cropped PCB defect dataset.

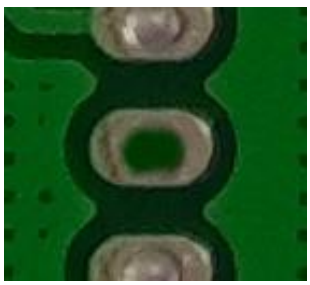
Defect Category	Number of Images
Missing hole	497
Mouse bite	492
Open circuit	482
Short circuit	491
Spur	488
Spurious copper	503
Total	**2953**

model's generalization ability, random horizontal and vertical flipping, affine transformations, and brightness–contrast adjustments were applied during training. The images were then normalized using the ImageNet mean and standard deviation to align with the pretrained weights for the MobileNetV3 architecture.

The data set was divided into training, validation, and test sets with a 70:15:15 split, and the number of images in each set was 2067, 443, and 443, respectively.

2.3 MobileNetV3-Based Classification Model

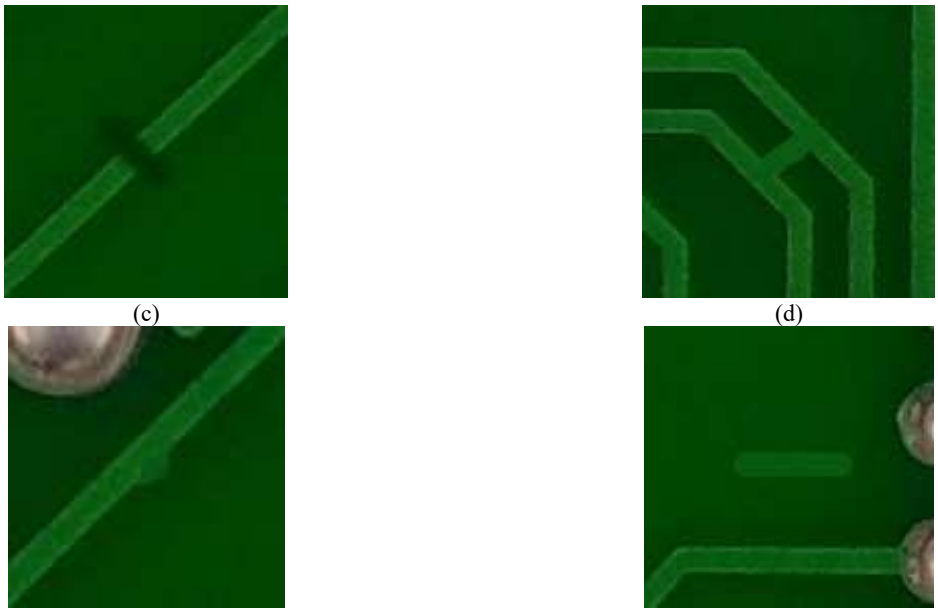
The MobileNetV3 network was selected as a backbone classification network due to its high accuracy, flexibility, and fast inference speed, making it suitable for intelligent industrial inspection systems [40]. It is built with depthwise separable convolutions, inverted residual bottleneck blocks, squeeze-and-excitation modules, and hardswish activation, which are not only efficient but also have competitive predictive performance. The overall classification pipeline used in this work, based on MobileNetV3, is shown in Figure 3.



(a)



(b)



(c) (d)

(e) (f)

Fig. 2: Cropped PCB defect images used for model training, including (a) Missing Hole, (b) Mouse Bite, (c) Open Circuit, (d) Short Circuit, (e) Spur, and (f) Spurious Copper.

The proposed framework follows a transfer learning approach, fine-tuning MobileNetV3 trained on the ImageNet dataset with the PCB defect dataset. The classification layer is replaced with a fully connected layer with 6 output neurons, each representing a different category of PCB defect. While training, all network parameters are optimized to adjust the pre-trained feature representations to the target domain.

For a given input image X, the feature representation extracted by the MobileNetV3 could be represented as:

$$\mathbf{f} = F(\mathbf{X}; \theta) \tag{1}$$

where $F(\cdot)$denotes the MobileNetV3 feature extraction network and θrepresents the learnable network parameters.

The extracted feature vector is subsequently mapped to the output layer through a fully connected classifier,

$$\mathbf{z} = W\mathbf{f} + b \tag{2}$$

where $W$and $b$denote the weight matrix and bias vector, respectively, while $z$represents the output logits.

The posterior probability corresponding to each PCB defect class is computed using the softmax activation function,

$$\boldsymbol{P(y = i|X)} = \frac{\mathbf{exp}(\boldsymbol{z_i})}{\sum_{j=1}^{C} \mathbf{exp}(\boldsymbol{z_j})} \tag{3}$$

where $C = 6$ denotes the total number of defect categories.

The network parameters are optimized by minimizing the cross-entropy loss with label smoothing,

$$\boldsymbol{\mathcal{L}} = -\sum_{\boldsymbol{i=1}}^{\boldsymbol{C}} \tilde{\boldsymbol{y}}_{\boldsymbol{i}} \mathbf{log}\big(\boldsymbol{P(y = i|X)}\big) \tag{4}$$

where

$$\tilde{y} = (1 - \varepsilon)y + \frac{\varepsilon}{C} \tag{5}$$

y denotes the ground-truth label, y represents the smoothed target distribution, and ε is the label smoothing coefficient.

The proposed framework automatically optimizes the learning rate, dropout rate, batch size, and fine-tuning configuration using the published TRIBRID optimization algorithm, eliminating the need for manual tuning. The optimized hyperparameters are then used to fine-tune the MobileNetV3 model, achieving better classification accuracy without empirical parameter tuning.

2.4 TRIBRID-Based Hyperparameter Optimization

The classification performance of deep learning models is highly dependent on the selection of training hyperparameters. Manual hyperparameter tuning is computationally expensive and often yields suboptimal configurations due to the nonlinear relationship between hyperparameters and model performance. To address this limitation, the published TRIBRID optimization algorithm [22] is employed to determine the optimal training hyperparameters of the MobileNetV3 classifier automatically.

In the proposed framework, each candidate solution represents a hyperparameter vector,

$$\mathbf{X} = [\eta,\ d,\ l,\ b], \tag{6}$$

where ηdenotes the learning rate, $d$represents the dropout rate, $l$corresponds to the number of trainable layers, and $b$denotes the batch size.

For every candidate solution, the MobileNetV3 model is trained using the selected hyperparameters, and the corresponding validation performance is evaluated. Since the objective of the optimization process is to maximize the classification performance, the optimization problem is formulated as

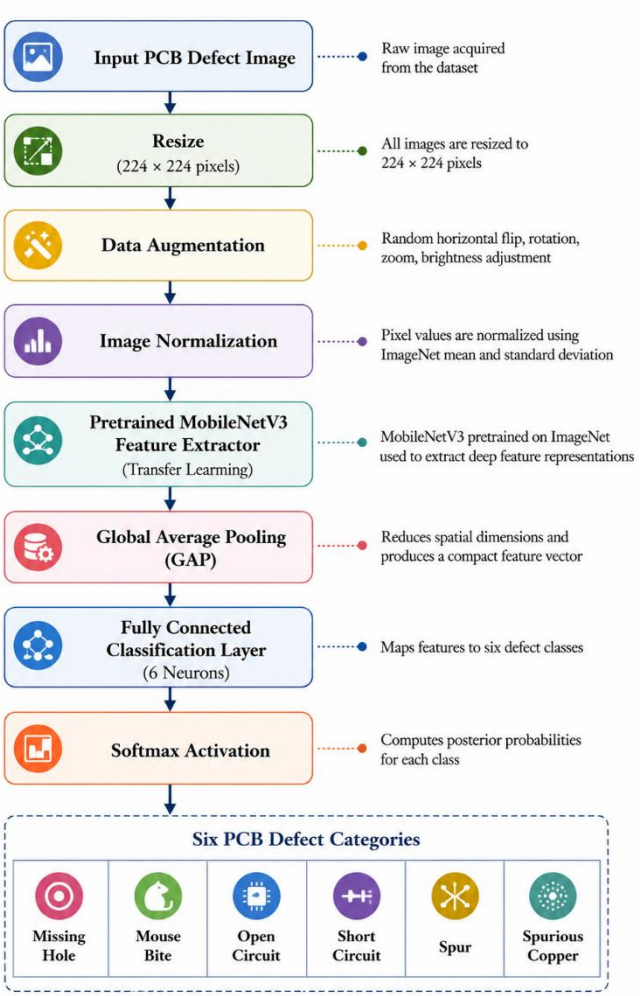


Fig 3: Architecture of the MobileNetV3-based PCB defect classification model adopted in the proposed framework.

$$\min f(\mathbf{X}) = 1 - F_1, \tag{7}$$

where F_1 denotes the macro-average F1-score computed on the validation dataset.

TRIBRID combines teacher-based learning, learner interaction, and scout-based exploration to balance global exploration and local exploitation during optimization. During the teacher phase, each candidate solution is updated according to the best-performing solution and the population mean,

$$\mathbf{X}_{new} = \mathbf{X}_i + r\left(\mathbf{X}_{best} - TF \cdot \overline{\mathbf{X}}\right), \tag{8}$$

where r is a uniformly distributed random number, TF denotes the teaching factor, $\boldsymbol{X}_{best}$ represents the current best solution, and X is the population mean.

During the learner phase, candidate solutions exchange information through pairwise interactions, allowing the search process to exploit promising regions of the solution space,

$$\mathbf{X}_{new} = \mathbf{X}_i + r\left(\mathbf{X}_i - \mathbf{X}_p\right), \tag{9}$$

where $\boldsymbol{X}_p$ denotes a randomly selected partner solution.

To avoid premature convergence, the scout phase introduces additional diversity through a Particle Swarm Optimization (PSO)-inspired search mechanism. The particle velocity is updated as

$$\mathbf{V}_i^{t+1} = w\mathbf{V}_i^t + c_1 r_1(\mathbf{P}_{best} - \mathbf{X}_i) + c_2 r_2(\mathbf{G}_{best} - \mathbf{X}_i), \tag{10}$$

where w denotes the inertia weight, c_1 and c_2 are the cognitive and social learning coefficients, respectively, while $\boldsymbol{P}_{best}$ and $\boldsymbol{G}_{best}$ represent the personal and global best solutions.

Finally, the optimized hyperparameter vector obtained by TRIBRID is employed to train the MobileNetV3 classifier using the complete training dataset. This automated optimization strategy improves convergence while reducing the dependence on empirical parameter selection. The overall optimization procedure adopted by the proposed framework is illustrated in Figure 4. Table 2 presents the search ranges of the hyperparameters optimized using the TRIBRID algorithm.

Table 2. Hyperparameter search space used by the TRIBRID optimization algorithm.

Hyperparameter	**Symbol**	**Search Range**
Learning rate	η	$(1 \times 10^{-4}) - (5 \times 10^{-3})$
Dropout rate	d	0.20 – 0.50
Trainable layers	l	1 – 15
Batch size	b	16 – 64

2.5 Explainable Classification Using Gradient-weighted Class Activation Mapping

The predictive mechanisms of deep learning models can be hard to interpret, even though their classification accuracy is high. To make the proposed framework more transparent, Grad-CAM was used to visualize the image regions that most strongly contribute to the predicted defect category [35]. Grad-CAM creates a class-discriminative localization map using gradients of the class with respect to the feature maps of the last convolutional layer.

For a target class c, the importance weight corresponding to the k^{th} feature map is computed as

$$\boldsymbol{\alpha_k^c} = \frac{\mathbf{1}}{\boldsymbol{Z}} \sum_{\boldsymbol{i}} \sum_{\boldsymbol{j}} \frac{\boldsymbol{\partial y^c}}{\boldsymbol{\partial A_{ij}^k}}, \tag{11}$$

where A_{ij}^k denotes the activation at spatial location (i, j) of the k^{th} feature map, y^c represents the class score before the Softmax layer, and Z is the total number of spatial locations.

The Grad-CAM localization map is subsequently obtained as

$$\boldsymbol{L_{\text{Grad-CAM}}^c} = \mathbf{ReLU}\left(\sum_{\boldsymbol{k}} \boldsymbol{\alpha_k^c A^k}\right), \tag{12}$$

where $\mathrm{ReLU}(\cdot)$ suppresses negative contributions and highlights the image regions that positively influence the

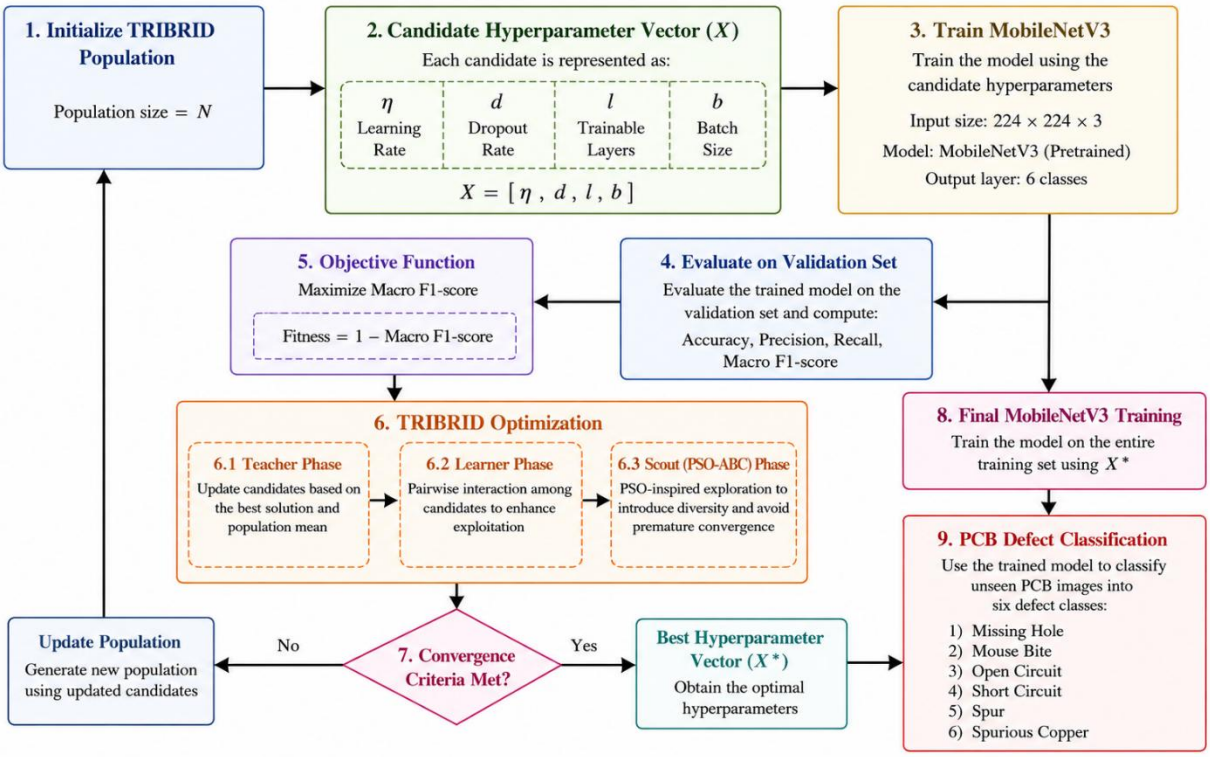


Fig 4: Workflow of the TRIBRID-based hyperparameter optimization process for automatic tuning of the MobileNetV3 classifier.

classification decision.

The obtained heatmaps were then overlaid on the original images of PCB defects to visualize the discriminative regions learned by the proposed model. By providing visual explanations, the classifiers can highlight specific defect areas rather than irrelevant background structures, thereby enhancing the interpretability and reliability of the proposed inspection framework.

3. Experimental Setup

3.1 Experimental Environment

The proposed framework has been implemented in Python using PyTorch, a deep learning framework version 2.11.0. Data augmentation and image preprocessing were performed using the Torchvision library, and the models were evaluated using the Scikit-learn package. The experiments were all run on a macOS 26.5.1 machine with an Apple Silicon processor and 32GB of RAM. All baseline and proposed models were trained and tested using a similar experimental setup to ensure a fair comparison.

3.2 Hyperparameter Settings

All experiments use the same training configuration, summarized in Table 3. To allow for a fair comparison, the same training setting was used for all baseline models, unless otherwise noted. The optimal hyperparameter values for the proposed framework were automatically determined using the TRIBRID optimization algorithm.

3.3 Performance Evaluation

The effectiveness of the proposed framework was tested using commonly used classification metrics, including Accuracy, Precision, Recall, F1-score, and Area Under the Receiver Operating Characteristic Curve (AUC). The metrics provide complementary information about the predictive ability and generalization performance of the classification

models.

$$\boldsymbol{Accuracy} = \frac{\boldsymbol{TP+TN}}{\boldsymbol{TP+TN+FP+FN}} \quad (\mathbf{13})$$

where TP, TN, FP, and FN denote the numbers of true positives, true negatives, false positives, and false negatives, respectively.

$$\boldsymbol{Precision} = \frac{\boldsymbol{TP}}{\boldsymbol{TP + FP}} \quad (\mathbf{14})$$

$$\boldsymbol{Recall} = \frac{\boldsymbol{TP}}{\boldsymbol{TP + FN}} \quad (\mathbf{15})$$

$$\boldsymbol{F_1} = \frac{\mathbf{2} \times \boldsymbol{Precision} \times \boldsymbol{Recall}}{\boldsymbol{Precision + Recall}} \quad (\mathbf{16})$$

To further evaluate the discriminative capability of the proposed framework, ROC curves and the corresponding AUC values were computed using the one-versus-rest strategy for the multiclass classification problem.

Table 3. Experimental configuration adopted for PCB defect classification.

Parameter	**Value**
Programming language	Python 3
Deep learning framework	PyTorch 2.11.0
Operating system	macOS 26.5.1 (Apple Silicon)
Processor	Apple Silicon (ARM)
System memory	32 GB
Input image size	224 × 224 pixels
Dataset split	70% Training : 15% Validation : 15% Testing
Data augmentation	Horizontal flip, Vertical flip, Affine transformation, Brightness–Contrast adjustment
Image normalization	ImageNet mean and standard deviation
Backbone network	MobileNetV3 (Transfer Learning)
Optimizer	AdamW
Loss function	Cross-Entropy Loss
Training epochs	40
Random seed	42
Population size (TRIBRID)	5
Maximum optimization iterations	5

In addition, confusion matrices were employed to analyze class-wise prediction performance, while Grad-CAM was used to provide visual interpretation of the learned defect representations.

4. Results and Discussion

4.1 Comparative Performance Analysis

The classification accuracy of the proposed framework was evaluated against four baseline frameworks: CNN, ResNet18, EfficientNet-B0, and baseline MobileNetV3. The quantitative results have been summarized in Table 4, and the accuracy of classification is shown in Figure 5.

Table 4. Comparative performance of the evaluated PCB defect classification models.

Model	Accuracy (%)	Precision (%)	Recall (%)	F1-score (%)
CNN	84.42	85.44	84.32	84.48
ResNet18	99.77	99.77	99.77	99.77
EfficientNet-B0	99.77	99.78	99.77	99.77
MobileNetV3	99.32	99.32	99.32	99.32
Proposed TRIBRID-MobileNetV3	**100.00**	**100.00**	**100.00**	**100.00**

As shown in Table 4, the custom CNN achieved 84.42% accuracy, indicating that shallow convolutional networks are not effective at learning the complex visual features of PCB surface defects. In contrast, all transfer-learning-based models achieved classification accuracies of more than 99%, demonstrating that the pretrained feature representation is effective for PCB defect classification. The base MobileNetV3 achieved a high accuracy of 99.32% with significantly lower computational complexity than ResNet18 and EfficientNet-B0, which both performed similarly at 99.77%.

The proposed TRIBRID-optimized MobileNetV3 framework achieved the highest performance across all evaluation metrics, with accuracy, precision, recall, and F1 score all at 100.00%. The proposed framework achieved 0.68 percentage points higher classification accuracy than the baseline model, MobileNetV3, demonstrating the effectiveness of intelligent hyperparameter optimization. While the overall improvement seems slight, it comes with no change to the network architecture or any increase in model complexity, indicating that proper hyperparameter tuning can greatly improve the learning ability of lightweight deep learning models.

Overall, the trend shown in Figure 5 aligns with the better performance of the proposed framework. The conversion of the CNN to transfer learning architectures led to a significant increase in classification accuracy. However, the TRIBRID optimization algorithm enabled MobileNetV3 to outperform the baseline models consistently. The results show that transfer learning, combined with intelligent hyperparameter optimization, is an effective approach for accurate, efficient classification of PCB defects.

4.2 Ablation Study

To assess the proposed TRIBRID optimization strategy, an ablation study was performed by comparing the baseline MobileNetV3 model with three hyperparameter optimization methods: Random Search, Particle Swarm Optimization (PSO), and the proposed TRIBRID.

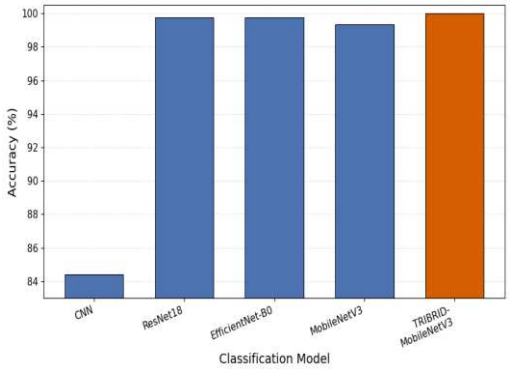


Fig 5: Comparative classification accuracy of the evaluated PCB defect classification models.

The training and evaluation conditions were identical across all experiments to ensure a fair comparison of the optimization strategies. The quantitative results are summarized in Tab. 5, and the accuracy comparison is shown in Fig. 6.

On the baseline MobileNetV3, the accuracy was 99.32%, as shown in Table 5, indicating that transfer learning is effective for PCB defect classification. Hyperparameter optimization further enhanced the model's performance, with 100.00% accuracy, precision, recall, and F1 score recorded for the three optimization techniques: Random search, PSO, and TRIBRID. The results show a significant improvement in the predictive capacity of the base model when the parameters are automatically optimized, compared to manually selecting the training parameters.

The classification performance of the three strategies was identical, but the sets of hyperparameters differed. Remarkably, the algorithm TRIBRID (proposed) had the best performance, and it needed to train 9 trainable layers, whereas the PSO had 15 layers, and the Random Search had 12 layers. This observation suggests that TRIBRID can retain a higher level of the pretrained feature extractor while preserving optimal classification accuracy, thereby minimizing the network adaptation needed for transfer learning.

The overall performance comparison in Figure 6 validates that hyperparameter optimization is significant for improving the capability of lightweight deep learning models for PCB defect classification.

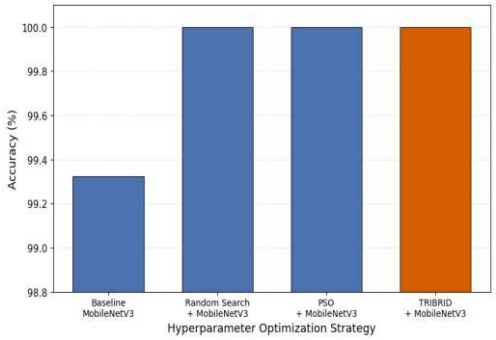


Fig 6: Performance comparison of different hyperparameter optimization strategies for MobileNetV3.

Moreover, the convergence behavior in Figure 4 shows that TRIBRID guides the optimization procedure to a desirable solution and maintains stable search behavior throughout the optimization iterations. The results indicate that the proposed framework achieves both the high computational efficiency of MobileNetV3 and a highly effective hyperparameter optimization strategy, making it applicable to resource-constrained industrial inspection systems.

4.3 Confusion Matrix Analysis

The confusion matrix is used to analyze the classification performance of the proposed framework, comparing predicted and actual defect categories for each class. The confusion matrix of the recommended TRIBRID-optimized MobileNetV3 model is displayed in Figure 7.

Table 5. Ablation study of different hyperparameter optimization strategies.

Hyperparameter Optimization Strategy	Trainable Layers	Accuracy (%)	Precision (%)	Recall (%)	F1-score (%)
Baseline MobileNetV3	10	99.32	99.33	99.32	99.32
Random Search + MobileNetV3	12	100.00	100.00	100.00	100.00
PSO + MobileNetV3	15	100.00	100.00	100.00	100.00
TRIBRID + MobileNetV3	**9**	**100.00**	**100.00**	**100.00**	**100.00**

As shown in Figure 7, the proposed framework accurately classified all six PCB defect categories: missing hole, mouse bite, open circuit, short circuit, spur, and spurious copper. The dominant diagonal elements indicate that all test samples were correctly classified in the ground truth, meaning no sample was misclassified during evaluation, and the absence of off-diagonal elements further supports this. The same can be seen in the quantitative performance shown in Table 4, where the proposed framework achieved 100.00% accuracy, precision, recall, and F1-score.

The confusion matrix also shows that the proposed classifier can correctly classify visually similar defect patterns, such as open circuit and short circuit, or spur and spurious copper defect, both of which are often difficult to distinguish due to their similar structural characteristics. The behavior suggests that transfer learning and hyperparameter optimization with TRIBRID can be used to learn highly discriminative feature representations for different categories of PCB defects.

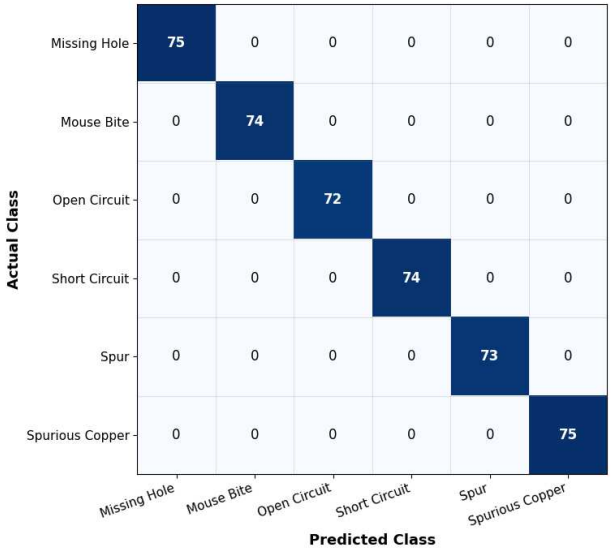


Fig 7: Confusion matrix of the proposed TRIBRID-optimized MobileNetV3 model for PCB defect classification.

In general, the confusion matrix results demonstrate the robustness and reliability of the proposed framework for multiclass PCB defect classification and further support its appropriateness for an intelligent AOI system.

4.4 ROC Analysis

To further assess the discriminative power of the proposed TRIBRID-optimized MobileNetV3 framework, the ROC curve was used. In the multiclass classification problem, ROC curves were generated using the one-versus-rest approach, and the AUC was calculated at both macro- and micro-average levels to provide an overall picture of classification performance. The obtained ROC curves are shown in Figure 8.

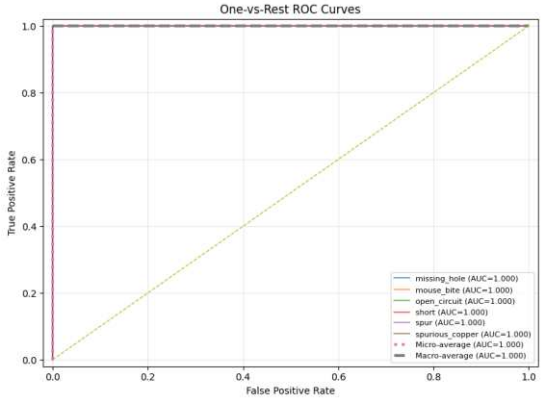


Fig 8: One-versus-rest ROC curves of the proposed TRIBRID-optimized MobileNetV3 model for PCB defect classification.

The ROC curves of all six categories of PCB defect are almost touching the top-left corner of the ROC space. This means that the classifiers are very good at separating the positive and negative classes. The proposed framework achieved an AUC of 1.0000 across all defect categories, a macro-average AUC of 1.0000, and a micro-average AUC of 1.0000. The results show that the classifier consistently assigns higher confidence scores to the correct defect category than to the other categories.

In addition, the ROC analysis is used to reinforce the confusion matrix shown in Figure 7, highlighting the great separability of the proposed framework in all defect categories. The combination of the confusion matrix and the ROC curves shows the high classification ability and reliability of the proposed model in multiclass PCB defect classification.

4.5 Explainability Analysis Using Gradient-weighted Class Activation Mapping

To make the proposed framework more interpretable, Grad-CAM was used to explain the discriminative image region that was involved in image classification. For each of the six PCB defect categories, representative images of the defects are shown, with the heatmap corresponding to those defect images in the right column, in Figure 9.

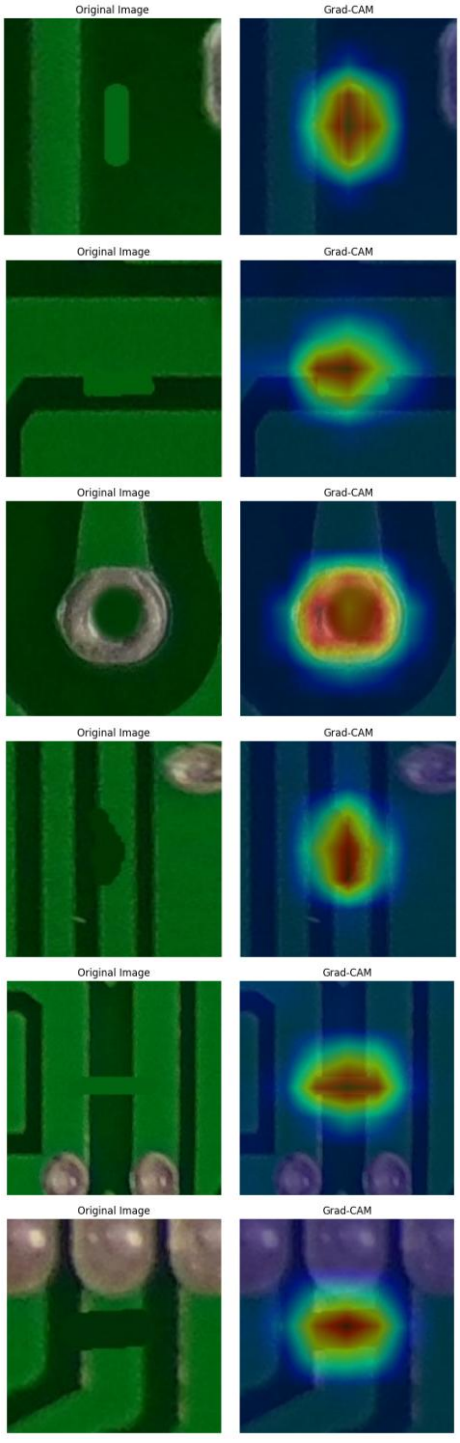


Fig 9: Grad-CAM visualizations for the six PCB defect categories.

The proposed framework always focuses on the specific defect regions, as shown in Figure 9, and not on the rest of the PCB background. The activation map accurately represents the circular defect area for the Missing Hole. At the same time, the Mouse Bite visualization highlights the irregular boundary deformation that causes the defect. Likewise, the activation maps for the two conditions, Open Circuit and Short Circuit, highlight the discontinuity (Open Circuit) and the unintended conductive connection (Short Circuit), respectively, demonstrating that the model captures the structural characteristics of electrical connectivity defects.

The Grad-CAM results for Spur and Spurious Copper also confirm the proposed approach's ability to localize the three-dimensional protruding conductive structures associated with each defect type. The high-intensity regions are linked to the faulty areas, which proves that the classifier is not using irrelevant background information to make predictions. This behavior provides additional confidence in the robustness of the learned feature representations.

4.5 Comparison with Recent PCB Defect Inspection Methods

The comparison shown in Table 6 indicates that recent research mainly focuses on full-image defect detection in PCBs using light CNNs, YOLO, or transformer architectures. The proposed TRIBRID-optimized MobileNetV3, on the other hand, obtains 100% accuracy, precision, recall, and F1-score in multiclass classification of cropped defect regions. It also includes auto-optimization of hyperparameters and Grad-CAM for interpretability, while maintaining computational efficiency and classification performance. However, the classification results do not need to be directly compared to the mAP results of an object detection method.

Table 6. Comparison of the proposed method with recent PCB defect inspection methods.

Method	Inspection task	Dataset / defect classes	Reported performance	Computational efficiency	Explainability
End-to-end single-stage deep-learning detector with multiscale feature extraction [1]	PCB defect localization and classification	HRIPCB/PKU-Market-PCB dataset; six defect classes	mAP@0.5 = 98.1%	7.02 M parameters; approximately three times fewer parameters than Faster R-CNN–ResNet-FPN and YOLOv5m	Not incorporated
Ensemble of two compact CNN-based detection models [4]	Industrial PCB defect reinspection and binary classification	Proprietary industrial dataset; normal and defective classes	Accuracy ≈ 95%; defective-class precision = 95.70%; recall = 94.29%	1.65 M parameters; 0.027 s per image	Not incorporated
LPViT transformer with label smoothing and masked-patch prediction [7]	PCB image classification and defect detection	PCB classification dataset and DeepPCB dataset	Detection mAP = 98.8%; classification speed reported as 156.1 FPS	Transformer architecture designed to balance classification performance and processing speed	Not incorporated
Lightweight deep-learning fusion model using MobileNetV3-Small, coordinate attention and multiscale feature fusion [18]	Small PCB defect detection and localization	Augmented public PCB dataset; six defect classes	Precision = 99.4%; recall = 97.6%; mAP = 99.0%	5.6 M parameters; 1.6 GFLOPs; 5.4 MB; 12.7 ms inference time; 78.73 FPS without image cutting	Coordinate-attention mechanism, but no post-hoc XAI method
YOLO-DTS with dual-branch Transformer extraction, deformable attention and spatial-attention detection head [21]	PCB defect detection in complex environments	PKU-Market-PCB; additionally evaluated on DeepPCB	Precision = 88.4%; recall = 69.9%; mAP50 = 77.5%	Parameters reduced by 13.4% compared with baseline YOLOv8	Attention modules are included, but no dedicated Grad-CAM explanation
Proposed TRIBRID-optimized MobileNetV3 with transfer learning and Grad-CAM	Classification of cropped PCB defect regions	Public PCB dataset; 2,953 cropped images; six defect classes	Accuracy = 100%; precision = 100%; recall = 100%; F1-score = 100%; AUC = 1.000	Lightweight MobileNetV3 backbone; nine trainable layers selected by TRIBRID	Grad-CAM explicitly visualizes the defect regions supporting each prediction

Overall, the proposed TRIBRID-optimized MobileNetV3 framework achieves high classification performance and produces interpretable decision-making, clearly showing the defect region responsible for each prediction. This level of

interpretability can be highly beneficial in industrial AOI applications, as it enables visual inspection of classification results, giving users added confidence and helping them troubleshoot issues.

5. Conclusion

This paper proposes a framework for classifying PCB defects using explainable automated methods based on the MobileNetV3 architecture optimized by TRIBRID. The proposed framework integrates transfer learning, lightweight deep learning, intelligent hyperparameter optimization, and XAI to enhance the accuracy and interpretability of PCB defect inspection. To test the proposed approach, a publicly available PCB defect dataset with 6 defect types was used. The proposed framework consistently achieved better classification results than a CNN, ResNet18, EfficientNet-B0, and the baseline MobileNetV3 model in comparative experiments. The ablation study also revealed a significant improvement in the base MobileNetV3 architecture through automatic hyperparameter optimization.

The proposed framework not only achieved high classification performance but also preserved the computational efficiency of MobileNetV3 and the number of layers to be optimized, which is less than that of other optimization methods. Additionally, the introduction of Grad-CAM enabled visualization of classification decisions and the identification of defect areas that led to each prediction. The results reported here show that the proposed framework is appropriate for intelligent AOI systems, where not only classification accuracy but also model transparency are crucial for reliable deployment in industry.

The framework proposed in this paper showed good performance on the dataset used in the experiments, but the experiments were performed with cropped defect regions from the annotated PCB images. The proposed framework will be further validated using image-level partitioning strategies and a larger industrial PCB dataset across various manufacturing scenarios in the future. Furthermore, the proposed framework can be extended to real-time defect detection, instance segmentation, and edge deployment, thereby further facilitating its application in next-generation intelligent manufacturing systems.

Author contributions:

Manjunath G. Asuti, Nirmalkumar S. Benni, Ramesh B T, Phanindra Reddy Kannari, Chaitra S N, Kavitha K J, B P Mishra have contributed to, read, and approved the manuscript in its current form. All authors conceived of the work, researched the necessary references, produced the scaling analysis, and wrote the manuscript together.

Funding:

This research received no external funding.

Data availability:

The datasets used or analyzed during the current study are available from the corresponding author on reasonable request.

Conflict of Interest:

The authors declare no conflict of interest.

Ethics Approval:

Not applicable. This study does not involve human participants or animals; therefore, ethical approval was not required.

The research is based purely on material fabrication and experimental analysis.

Consent to Participate:

Not applicable. The study does not involve any human subjects or participants requiring consent.

Consent to Publish:

Not applicable. No individual or personal data is included in this study that requires consent for publication.

Clinical trial number:

Not applicable.

References

1) Bhattacharya, Abhiroop, and Sylvain G. Cloutier. "End-to-end deep learning framework for printed circuit board manufacturing defect classification." *Scientific Reports* 12, no. 1 (2022): 12559.
2) Ling, Qin, and Nor Ashidi Mat Isa. "Printed circuit board defect detection methods based on image processing, machine learning and deep learning: A survey." *IEEE Access* 11 (2023): 15921-15944.
3) Chen, Xing, Yonglei Wu, Xingyou He, and Wuyi Ming. "A comprehensive review of deep learning-based PCB defect detection." *IEEE Access* 11 (2023): 139017-139038.
4) Chen, I-Chun, Rey-Chue Hwang, and Huang-Chu Huang. "PCB defect detection based on deep learning algorithm." *Processes* 11, no. 3 (2023): 775.
5) Lv, Shengping, Bin Ouyang, Zhihua Deng, Tairan Liang, Shixin Jiang, Kaibin Zhang, Jianyu Chen, and Zhuohui Li. "A dataset for deep learning based detection of printed circuit board surface defect." *Scientific Data* 11, no. 1 (2024): 811.
6) Legon, Andria, Makarand Deo, Sacharia Albin, and Michel Audette. "Detection and classification of PCB defects using deep learning methods." In *2022 IEEE 31st Microelectronics Design & Test Symposium (MDTS)*, pp. 1-6. IEEE, 2022.
7) An, Kang, and Yanping Zhang. "LPViT: A transformer based model for PCB image classification and defect detection." *IEEE Access* 10 (2022): 42542-42553.
8) Nguyen, Van-Truong, and Huy-Anh Bui. "A real-time defect detection in printed circuit boards applying deep learning." *EUREKA: Physics and Engineering* 2 (2022): 143-153.
9) Kaya, Gulhan Ustabas. "Development of hybrid optical sensor based on deep learning to detect and classify the micro-size defects in printed circuit board." *Measurement* 206 (2023): 112247.
10) Sharma, Aryan, Manan Agrawal, Parikshit Sardeshpande, Aditya Gupta, Ayaan Pasha, and Richa R. Khandelwal. "PCB defect detection using deep learning methods." In *2024 15th International Conference on Computing Communication and Networking Technologies (ICCCNT)*, pp. 1-7. IEEE, 2024.
11) Pham, Thi Tram Anh, Do Kieu Trang Thoi, Hyohoon Choi, and Suhyun Park. "Defect detection in printed circuit boards using semi-supervised learning." *Sensors* 23, no. 6 (2023): 3246.
12) Lim, JiaYou, JunYi Lim, Vishnu Monn Baskaran, and Xin Wang. "A deep context learning based PCB defect detection model with anomalous trend alarming system." *Results in Engineering* 17 (2023): 100968.
13) Yu, Xinyi, Li Han-Xiong, and Haidong Yang. "Collaborative learning classification model for PCBs defect detection against image and label uncertainty." *IEEE Transactions on Instrumentation and Measurement* 72 (2023): 1-8.
14) Kaya, Volkan, and İsmail Akgül. "Detection of defects in printed circuit boards with machine learning and deep learning algorithms." *Avrupa Bilim ve Teknoloji Dergisi* 41 (2022): 183-186.
15) Liu, Yaojun, Ping Wang, Jingjing Liu, and Chuanyang Liu. "X-ray PCB defect automatic diagnosis algorithm based on deep learning and artificial intelligence." *Neural Computing and Applications* 35, no. 36 (2023): 25263-25273.
16) Chi, Tay Shiek, Mohd Nadhir Ab Wahab, Ahmad Sufril Azlan Mohamed, Mohd Halim Mohd Noor, Khaw Beng Kang, Lim Lay Chuan, and Liau Wei Jie Brigitte. "Enhancing EfficientNet-YOLOv4 for integrated circuit detection on printed circuit board (PCB)." *IEEE Access* 12 (2024): 25066-25078.
17) LIKITHA, SAI, GUTTI PRADEEP, and CHALLAGULLA BHAVYA SRI. "Deep Learning-Based PCB Defect Detection Using Enhanced Faster R-CNN and MobileNet." *Journal of Nonlinear Analysis and Optimization* 16, no. 1 (2025).
18) Wang, Yuling, Zhicheng Chen, Jie Wang, Peng Shang, Arcot Sowmya, and Changming Sun. "Printed Circuit Board Defect Detection Based on Lightweight Deep Learning Fusion Model." *Sensors* 25, no. 24 (2025): 7403.
19) Zhao, Qian, Tangyu Ji, Shuang Liang, and Wentao Yu. "PCB surface defect fast detection method based on attention and multi-source fusion." *Multimedia Tools and Applications* 83, no. 2 (2024): 5451-5472.
20) Tang, Zhe, Xin Xiong, Hui Lan, and Xi Hu. "YOLO-MDMN: A new lightweight algorithm for efficient PCB defect detection." *Measurement Science and Technology* 37, no. 9 (2026): 095003.
21) Ou, Yufeng, and Chia-Hung Wang. "A transformer-based dual-branch feature extraction for printed circuit board defect detection with enhanced spatial attention mechanism." *Applied Soft Computing* (2025): 114072.
22) Suman, Abhineet, Gunjan Rehani, and Sandeep S. Udmale. "A novel optimized remaining useful life forecasting model for lithium-ion batteries." *Evolving Systems* 17, no. 2 (2026): 38.
23) Chowdhury, Anjir Ahmed, Argho Das, Khadija Kubra Shahjalal Hoque, and Debajyoti Karmaker. "A comparative study of hyperparameter optimization techniques for deep learning." In *Proceedings of the International Joint Conference on Advances in Computational Intelligence (IJCACI 2021)*, pp. 509-521. Springer, 2022.
24) Wojciuk, Mikolaj, Zaneta Swiderska-Chadaj, Krzysztof Siwek, and Arkadiusz Gertych. "Improving classification accuracy of fine-tuned CNN models: Impact of hyperparameter optimization." *Heliyon* 10, no. 5 (2024).

25) Yaloveha, Vladyslav, Andrii Podorozhniak, and Heorhii Kuchuk. "Convolutional neural network hyperparameter optimization applied to land cover classification." *Radioelectronic and Computer Systems* 1 (2022): 115-128.
26) Liao, Lizhi, Heng Li, Weiyi Shang, and Lei Ma. "An empirical study of the impact of hyperparameter tuning and model optimization on the performance properties of deep neural networks." *ACM Transactions on Software Engineering and Methodology* 31, no. 3 (2022): 1-40.
27) Aguerchi, Khadija, Younes Jabrane, Maryam Habba, and Amir Hajjam El Hassani. "A CNN hyperparameters optimization based on particle swarm optimization for mammography breast cancer classification." *Journal of Imaging* 10, no. 2 (2024): 30.
28) Raji, Ismail Damilola, Habeeb Bello-Salau, Ime Jarlath Umoh, Adeiza James Onumanyi, Mutiu Adesina Adegboye, and Ahmed Tijani Salawudeen. "Simple deterministic selection-based genetic algorithm for hyperparameter tuning of machine learning models." *Applied Sciences* 12, no. 3 (2022): 1186.
29) Rimal, Yagyanath, Navneet Sharma, and Abeer Alsadoon. "The accuracy of machine learning models relies on hyperparameter tuning: student result classification using random forest, randomized search, grid search, Bayesian, genetic, and Optuna algorithms." *Multimedia Tools and Applications* 83, no. 30 (2024): 74349-74364.
30) Kazi, Aafreen, and Siba Prasada Panda. "Determining the freshness of fruits in the food industry by image classification using transfer learning." *Multimedia Tools and Applications* 81, no. 6 (2022): 7611-7624.
31) Ma, Guijun, Songpei Xu, Tao Yang, Zhenbang Du, Limin Zhu, Han Ding, and Ye Yuan. "A transfer learning-based method for personalized state of health estimation of lithium-ion batteries." *IEEE Transactions on Neural Networks and Learning Systems* 35, no. 1 (2022): 759-769.
32) Zhong, Hongyu, Samson Yu, Hieu Trinh, Yong Lv, Rui Yuan, and Yanan Wang. "Fine-tuning transfer learning based on DCGAN integrated with self-attention and spectral normalization for bearing fault diagnosis." *Measurement* 210 (2023): 112421.
33) Li, Chuanjiang, Shaobo Li, Huan Wang, Fengshou Gu, and Andrew D. Ball. "Attention-based deep meta-transfer learning for few-shot fine-grained fault diagnosis." *Knowledge-Based Systems* 264 (2023): 110345.
34) Subramanian, Malliga, Kogilavani Shanmugavadivel, and P. S. Nandhini. "On fine-tuning deep learning models using transfer learning and hyper-parameters optimization for disease identification in maize leaves." *Neural Computing and Applications* 34, no. 16 (2022): 13951-13968.
35) Satsangi, Aditi, Prem Prakash Vuppuluri, and Gurumukh Das. "Explainable deep learning approaches for classifying welding defects—Integrating CNN architectures with XAI." *International Journal on Interactive Design and Manufacturing (IJIDeM)* 20, no. 3 (2026): 1433-1456.
36) Kim, Ho-Seung, Jiho Jung, Ryul Hwang, Seong-Chan Park, Seung-Jae Lee, Gyu-Tae Kim, and Bang-Wook Lee. "Classification of PRPD pattern in cast-resin transformers using CNN and implementation of Explainable AI (XAI) with Grad-CAM." *IEEE Access* 12 (2024): 53623-53632.
37) Saleh, Radhwan A. A., and H. Metin Ertunç. "Explainable attention-based fused convolutional neural network (XAFCNN) for tire defect detection: An industrial case study." *Engineering Research Express* 6, no. 1 (2024): 015090.
38) Selvaraju, Ramprasaath R., Michael Cogswell, Abhishek Das, Ramakrishna Vedantam, Devi Parikh, and Dhruv Batra. "Grad-CAM: Visual explanations from deep networks via gradient-based localization." In *Proceedings of the IEEE International Conference on Computer Vision (ICCV)*, pp. 618-626. 2017.
39) Aboulhosn, Zeina, Ahmad Musamih, Khaled Salah, Raja Jayaraman, Mohammed Omar, and Zeyar Aung. "Detection of manufacturing defects in steel using deep learning with explainable artificial intelligence." *IEEE Access* 12 (2024): 99240-99257.
40) Howard, Andrew, Mark Sandler, Grace Chu, Liang-Chieh Chen, Bo Chen, Mingxing Tan, Weijun Wang, et al. "Searching for MobileNetV3." In *Proceedings of the IEEE/CVF International Conference on Computer Vision (ICCV)*, pp. 1314-1324. 2019.
41) Tan, Mingxing, and Quoc Le. "EfficientNet: Rethinking model scaling for convolutional neural networks." In *Proceedings of the International Conference on Machine Learning (ICML)*, pp. 6105-6114. PMLR, 2019.